NASA TECHNICAL NOTE

NASA TN D-7339

NASA TN D-7339

NUMERICAL SIMULATION OF NOISE PROPAGATION IN JET ENGINE DUCTS

by Kenneth J. Baumeister and Edward C. Bittner

Lewis Research Center
Cleveland, Ohio 44135

NATIONAL AERONAUTICS AND SPACE ADMINISTRATION • WASHINGTON, D. C. • OCTOBER 1973

1. Report No.	2. Government Accession No.	3. Recipient's Catalog No.
NASA TN D-7339		

4. Title and Subtitle	5. Report Date
NUMERICAL SIMULATION OF NOISE PROPAGATION IN JET ENGINE DUCTS	October 1973
	6. Performing Organization Code

7. Author(s)	8. Performing Organization Report No.
Kenneth J. Baumeister and Edward C. Bittner	E-7217
	10. Work Unit No. 501-04

9. Performing Organization Name and Address	11. Contract or Grant No.
Lewis Research Center National Aeronautics and Space Administration Cleveland, Ohio 44135	
	13. Type of Report and Period Covered Technical Note
12. Sponsoring Agency Name and Address National Aeronautics and Space Administration Washington, D. C. 20546	14. Sponsoring Agency Code

15. Supplementary Notes

16. Abstract

A finite difference formulation is presented which should be useful in the study of acoustically treated inlet and exhaust ducts used in turbofan engines. The difference formulation can readily handle acoustic flow field complications, such as axial variations in wall impedance and cross-sectional area, that would occur in a sonic inlet. In formulating the difference solutions, the continuous acoustic field is lumped into a series of grid points spread uniformly throughout the field. At each point, the pressure is separated into its real and imaginary terms. Example solutions are presented for sound propagation in a one-dimensional straight hard-wall duct and in a two-dimensional straight soft-wall duct without steady flow.

17. Key Words (Suggested by Author(s))		18. Distribution Statement
Acoustic	Ducts	Unclassified - unlimited
Suppressor	Turbofan	
Finite difference		

19. Security Classif. (of this report)	20. Security Classif. (of this page)	21. No. of Pages	22. Price*
Unclassified	Unclassified	48	Domestic, $3.00 Foreign, $5.50

* For sale by the National Technical Information Service, Springfield, Virginia 22151

CONTENTS

NUMERICAL SIMULATION OF NOISE PROPAGATION IN JET ENGINE DUCTS

by Kenneth J. Baumeister and Edward C. Bittner

Lewis Research Center

SUMMARY

A finite difference formulation is presented which should be useful in the study of acoustically treated inlet and exhaust ducts used in turbofan engines. The difference formulation can readily handle acoustic flow field complications, such as axial variations in wall impedance and cross-sectional area, that would occur in a sonic inlet. The formulation is both mathematically rigorous and convenient to use.

In formulating the difference solutions, the continuous acoustic field is lumped into a series of grid points spread uniformly throughout the acoustic field. At each grid point in the acoustic field, the pressure is separated into its real and imaginary terms. Then, the two-dimensional Helmholtz equations for both the real and imaginary pressures at each grid point are expressed in difference form. The solution is obtained by coupling the difference equations for the real and imaginary pressures with the impedance conditions at the boundaries. The solution yields the two-dimensional distribution of pressure, velocity, and intensity level throughout the duct.

The coefficient matrix of the acoustic difference equations is presented and discussed. Then, example solutions are presented for the propagation of sound in a one-dimensional straight hard-wall duct and in a two-dimensional straight soft-wall duct without steady flow. These numerical solutions showed favorable comparison with the exact analytical results. The examples are used to establish rules of thumb for choosing grid sizes for various frequencies and duct lengths.

Because the solution matrix for the acoustic flow field is not positive definite, conventional iteration techniques cannot be used to solve the difference equations. Before the finite difference formulation can be applied to more complicated problems which require a large number of grid points, such as the sonic inlet, iteration techniques will have to be developed to overcome present grid-size limitations.

INTRODUCTION

The level of noise currently being proposed for new aircraft requires the use of acoustic suppression in the inlet and outlet ducts of their engines. At the present time, there is a need for more flexible suppressor design techniques which can handle acoustic flow field complications in engine ducts, such as axial variations in wall impedance and cross-sectional area, that would occur in a sonic inlet. To meet this need, the present report develops a numerical finite difference technique which can be used in the prediction of sound attenuation in turbojet engine ducts. In addition, acoustic wave propagation is important in ultrasonics and underwater technology, as well as in conventional noise abatement problems in archtitectural engineering. The techniques presented herein might also be applied to these other areas of acoustics.

Morse (ref. 1), Cremer (ref. 2), and Rice (ref. 3) have presented analytical solutions for the transmission of sound in ducts of infinite length, uniform cross section, constant wall impedance, and no flow. The theoretical solutions were later extended by Rice (ref. 4), Eversman (ref. 5), and Lambert and Tack (ref. 6) to acoustic propagation with uniform subsonic flows. Pridmore-Brown (ref. 7), as well as other authors (refs. 8 to 17), has shown that shear flows (boundary-layer effects) can have a significant influence on the attenuation of sound in ducts. All these works use the technique of separation of variables to obtain a complex eigenvalue formulation in which the eigenvalues are determined by various numerical techniques.

The present report formulates a solution for the propagation of sound in ducts with arbitrary wall impedance by a finite difference technique. A search of the literature failed to uncover any previous work in this area. The difference solutions bypass the conventional eigenvalue problem with its associated modes. As a result of the difference formulation, the propagation of noise is treated as a diffusion process analogous to problems in thermodynamics involving heat flow or those in fluid dynamics involving the transport of vorticity.

Immediately following the mathematical development of the difference technique, two examples are presented to illustrate the numerical technique. These examples have analytical solutions; therefore, a direct comparison between the numerical and analytical results can be made. These examples are also used to establish rules of thumb for choosing grid sizes for various frequencies and duct lengths. By choosing the maximum acceptable grid size, the amount of computer time necessary to obtain a solution to the finite difference equations can be minimized.

The first example presents a solution for the sound propagation in a one-dimensional hard-wall duct with the impedance specified at the duct exit. The second example treats the propagation in a two-dimensional straight soft-wall duct without steady flow. Also, the limitations of the present theory are discussed and suggestions for future work are presented.

GOVERNING EQUATION AND BOUNDARY CONDITIONS

The governing differential equation and boundary conditions are introduced in this section of the report. First, the equations are presented in dimensional form. Next, the equations are made nondimensional, and the significance of the dimensionless parameters is briefly discussed.

The basic equations for the scalar pressure field and the velocity field are presented, as well as the appropriate expressions for the wall impedance condition and acoustical intensity.

Scalar Pressure Field

The continuity, momentum, energy, and state equations of a perfect gas in a duct reduce, in the case of no steady flow, to the linear two-dimensional wave equation

$$\nabla'^2 P' = \frac{1}{c^2} \frac{\partial^2 P'}{\partial t^2} \tag{1}$$

In equation (1), c is the speed of sound, t is time, and P' is the pressure fluctuation which is assumed to be small compared to the ambient pressure. The prime (') is used to denote a dimensional quantity. (These and all other symbols used in this report are defined in appendix A.)

The assumptions involved in the derivation of equation (1) are given in most acoustic texts and are not discussed herein. For ease in illustrating the numerical techniques, we have chosen this simple form of the wave equation rather than the more complete form, which contains Mach number and shear flow effects such as given by Mungur and Gladwell (ref. 8).

We now make a further simplification by working in rectangular coordinates. In this case, equation (1) can be expressed as

$$\frac{\partial^2 P'}{\partial x'^2} + \frac{\partial^2 P'}{\partial y'^2} = \frac{1}{c^2} \frac{\partial^2 P'}{\partial t^2} \tag{2}$$

where

$$P' = P'(x', y', t) \tag{3}$$

This coordinate system is illustrated in figure 1.

We are concerned primarily with the steady-state solutions of the wave equation, equation (2); consequently, we neglect the transient startup effects in the system. Thus, for steady state we assume a solution of the form

$$P'(x',y',t) = p'(x',y')e^{+i\omega t} \tag{4}$$

where in general

$$p'(x',y') = p'^{(1)}(x',y') + ip'^{(2)}(x',y') \tag{5}$$

The (1) and (2) superscripts designate the real and imaginary pressure components. Both $p'^{(1)}$ and $p'^{(2)}$ are real-valued functions by definition. Complex quantities are used because of the ease of manipulation; however, only the real part of the solution will have physical significance. Substituting equation (4) into the scalar wave equation (eq. (2)) yields

$$\frac{\partial^2 p'}{\partial x'^2} + \frac{\partial^2 p'}{\partial y'^2} + k^2 p' = 0 \tag{6}$$

where the wave number k is given by

$$k = \frac{\omega}{c} \tag{7}$$

Equation (6) is commonly called the Helmholtz equation. This equation and its appropriate boundary conditions will be solved numerically by the finite difference technique.

In nondimensionalizing equation (6) we choose to write equation (6) in such a form that the numerical results will be compatible with present NASA Lewis acoustical design procedures. To do this, we define the following set of dimensionless variables as suggested by the results of Rice (ref. 4):

$$y = \frac{y'}{H} \tag{8}$$

$$x = \frac{x'}{H} \tag{9}$$

$$p = \frac{p'}{p_A} \tag{10}$$

where H equals the height of the rectangular duct and p_A will usually be chosen as the amplitude of the imposed pressure wave at $x = 0$.

Substituting equations (8) to (10) into equation (6) and rearranging terms gives

$$\frac{\partial^2 p}{\partial x^2} + \frac{\partial^2 p}{\partial y^2} + (2\pi\eta)^2 p = 0 \tag{11}$$

where

$$\eta = \frac{H}{2\pi}\frac{\omega}{c} = \frac{Hf}{c} = \frac{H}{\lambda} \tag{12}$$

The frequency parameter η represents the ratio of duct height to acoustic wavelength. The dimensionless height y ranges from zero to 1, while the dimensionless length x ranges between

$$0 \leq x \leq \frac{L}{H} \tag{13}$$

where L is the length of the duct. Thus, the important dimenionless parameters describing the acoustic attenuation are η and L/H.

Equation (11) now can be broken into its real and imaginary parts. Substituting equation (5) into equation (11) yields

$$\frac{\partial^2 p^{(1)}}{\partial x^2} + \frac{\partial^2 p^{(1)}}{\partial y^2} + (2\pi\eta)^2 p^{(1)} = 0 \tag{14}$$

$$\frac{\partial^2 p^{(2)}}{\partial x^2} + \frac{\partial^2 p^{(2)}}{\partial y^2} + (2\pi\eta)^2 p^{(2)} = 0 \tag{15}$$

Acoustic Particle Velocity

The boundary conditions in acoustics are generally given in terms of impedances

which relate the pressure and velocity fields at the boundary. The velocity field can be expressed in terms of pressure from the equation

$$\rho\left(\frac{\partial \bar{u}'}{\partial t}\right) = -\nabla' P' \tag{16}$$

which for a harmonic solution of the form given by equation (4) reduces to

$$\bar{u}' = \frac{i}{\rho\omega} \nabla' p' \tag{17}$$

In terms of the scalar velocities, equation (17) becomes

$$u_x' = \frac{i}{\rho\omega} \frac{\partial p'}{\partial x'} \tag{18}$$

$$u_y' = \frac{i}{\rho\omega} \frac{\partial p'}{\partial y'} \tag{19}$$

In terms of the dimensionless parameters, equations (18) and (19) become

$$u_x = i \frac{\partial p}{\partial x} \tag{20}$$

$$u_y = i \frac{\partial p}{\partial y} \tag{21}$$

where

$$\bar{u} = \frac{\rho\omega H}{p_A} \bar{u}' \tag{22}$$

Impedance Boundary Condition

In the transverse direction, the acoustic impedance at the walls is defined as

$$Z_t = \frac{p'}{u_y'} \quad \text{at } y = 0 \text{ and } 1 \tag{23}$$

The impedance Z_t is now replaced by the impedance ratio ζ_t, which is defined as

$$\zeta_t = \frac{Z_t}{\rho c} \tag{24}$$

Substituting equation (19) into (23) and introducing the dimensionless parameters yield the following expression for the impedance at the walls:

$$\zeta_t = -i2\pi\eta \frac{p}{\frac{\partial p}{\partial y}} \quad \text{at } y = 0 \text{ and } 1 \tag{25}$$

or, the pressure gradients at the walls become

$$\frac{\partial p}{\partial y} = \frac{-i2\pi\eta}{\zeta_t} p \quad \text{at } y = 0 \text{ and } 1 \tag{26}$$

Because of convenience, we shall use equation (26) to apply the boundary constraint rather than equation (25).

It is convenient to express the reciprocal of the impedance ratio in terms of the acoustic conductance ratio κ_t and the acoustic susceptance ratio σ_t, that is,

$$\frac{1}{\zeta_t} \equiv \kappa_t - i\sigma_t \tag{27}$$

where $1/\zeta_t$ is called the acoustic admittance ratio. Therefore, equation (26) becomes

$$\frac{\partial p}{\partial y} = -2\pi\eta(\sigma_t + i\kappa_t) p \tag{28}$$

Finally, expressing p in terms of its real and imaginary terms, and equating these terms gives

$$\frac{\partial p^{(1)}}{\partial y} = -2\pi\eta\left[p^{(1)}\sigma_t - p^{(2)}\kappa_t\right] \quad \text{at } y = 0 \text{ and } 1 \tag{29}$$

$$\frac{\partial p^{(2)}}{\partial y} = -2\pi\eta\left[p^{(2)}\sigma_t + p^{(1)}\kappa_t\right] \quad \text{at } y = 0 \text{ and } 1 \tag{30}$$

The impedance at the exit plane, $x = L/H$, leads to a similar expression

$$\left.\frac{\partial p^{(1)}}{\partial x}\right]_{x=L/H} = -2\pi\eta\left[p^{(1)}\sigma_e - p^{(2)}\kappa_e\right] \tag{31}$$

$$\left.\frac{\partial p^{(2)}}{\partial x}\right]_{x=L/H} = -2\pi\eta\left[p^{(2)}\sigma_e + p^{(1)}\kappa_e\right] \tag{32}$$

We can see that the pressures $p^{(1)}$ and $p^{(2)}$ are coupled by the impedance conditions represented by equations (29) to (32).

Entrance Conditions

At the entrance, the dimensionless pressure $p(0,y)$ is assumed to be of a general form

$$p(0,y) = p^{(1)}(0,y) + ip^{(2)}(0,y) \tag{33}$$

Generally, some real pressure profile $f(y)$ is assumed at the entrance, that is

$$p(0,y) = f(y) \tag{34}$$

where $f(y)$ is normalized such that

$$\int_0^1 f(y)dy = 1 \tag{35}$$

The function $f(y)$ can be chosen to map any assumed pressure profile. For the problems treated in this report, the real and imaginary pressures at $x = 0$ are

$$p^{(1)}(0,y) = f(y) \tag{36}$$

$$p^{(2)}(0,y) = 0 \tag{37}$$

For a uniform profile, as is used in the examples considered later, equation (36) becomes

$$p^{(1)}(0,y) = 1 \tag{38}$$

Axial Acoustic Power

The sound power which leaves a duct and reaches the far field is related to the axial intensity. The axial intensity can be expressed as (ref. 4)

$$I' = \frac{1}{2} \mathcal{R}e \left\{ p^{*\prime} u_x' \right\} \tag{39}$$

In terms of the dimensionless parameters, equation (39) can be written in dimensionless form as

$$I = \frac{1}{2\pi\eta} \mathcal{R}e \left\{ p^* u_x \right\} \tag{40}$$

where

$$I = \frac{2\rho c}{p_A^2} I' \tag{41}$$

For a hard-wall duct with a ρc exit impedance, I is identical to 1 for all frequencies and duct lengths. This result is shown in appendix B.

In terms of the complex representation, the expression for I becomes

$$I = \frac{1}{2\pi\eta} \left[p^{(2)} \frac{\partial p^{(1)}}{\partial x} - p^{(1)} \frac{\partial p^{(2)}}{\partial x} \right] \tag{42}$$

The total dimensionless acoustic power is the integral of the intensity across the test section

$$E_x = \int_0^1 I(x,y)dy \tag{43}$$

By definition the decrease in decibels of the acoustic power from $x = 0$ to x can be written as

$$\Delta dB = 10 \log_{10} \frac{E_x}{E_0} \tag{44}$$

FINITE DIFFERENCE FORMULATION

The continuous system will now be reduced to an equivalent lumped-parameter system by means of the finite difference approximations. Instead of a continuous solution for the pressure, we shall find the pressure at isolated grid points, as shown in figure 2.

The previously discussed governing differential equations can be approximated in difference form (ref. 18) by using one of the following three methods: (1) a Taylor series expansion, (2) a variational formulation, or (3) an integral formulation. For problems where the gradient is specified along a boundary, such as in our acoustic problem, the integration method for generating the finite difference approximations is most convenient and is used in this report.

The difference equations for the acoustic field are presented without derivation. The detailed derivations of these equations are given in appendixes C and D.

Helmholtz Equation

The Helmholtz equation, (14), in finite difference form becomes

$$-p^{(1)}_{i-1,j} - p^{(1)}_{i+1,j} - \left(\frac{\Delta x}{\Delta y}\right)^2 \left[p^{(1)}_{i,j-1} + p^{(1)}_{i,j+1}\right] + \left[2 + 2\left(\frac{\Delta x}{\Delta y}\right)^2 - (2\pi\eta\ \Delta x)^2\right] p^{(1)}_{i,j} = 0 \tag{45}$$

$$-p^{(2)}_{i-1,j} - p^{(2)}_{i+1,j} - \left(\frac{\Delta x}{\Delta y}\right)^2 \left[p^{(2)}_{i,j-1} + p^{(2)}_{i,j+1}\right] + \left[2 + 2\left(\frac{\Delta x}{\Delta y}\right)^2 - (2\pi\eta\ \Delta x)^2\right] p^{(2)}_{i,j} = 0 \tag{46}$$

where

$$p_{i,j} = p^{(1)}_{i,j} + i p^{(2)}_{i,j} \tag{47}$$

and where i corresponds to x and j corresponds to y. Note, the frequency term

$(2\pi\eta\ \Delta x)^2$ subtracts from the term which will occupy the main diagonal element of the coefficient matrix; consequently, for sufficiently high frequencies or spacing parameters, the matrix will no longer be positive definite (ref. 18, p. 68). As a result, conventional iteration techniques cannot be used.

Impedance Boundary Conditions

The impedance boundary conditions of the upper wall with $j = m$ (eqs. (29) and (30)) become

$$p_{i,m}^{(1)}\left[1 + \left(\frac{\Delta y}{\Delta x}\right)^2 + 2\pi\eta\ \Delta y \left(\sigma_t\right)_{i,m} - \frac{(2\pi\eta\ \Delta y)^2}{2}\right] - p_{i,m-1}^{(1)} - \frac{1}{2}\left(\frac{\Delta y}{\Delta x}\right)^2 p_{i-1,m}^{(1)}$$

$$- \frac{1}{2}\left(\frac{\Delta y}{\Delta x}\right)^2 p_{i+1,m}^{(1)} - 2\pi\eta\ \Delta y \left(\kappa_t\right)_{i,m} p_{i,m}^{(2)} = 0 \tag{48}$$

$$p_{i,m}^{(2)}\left[1 + \left(\frac{\Delta y}{\Delta x}\right)^2 + 2\pi\eta\ \Delta y \left(\sigma_t\right)_{i,m} - \frac{(2\pi\eta\ \Delta y)^2}{2}\right] - p_{i,m-1}^{(2)} - \frac{1}{2}\left(\frac{\Delta y}{\Delta x}\right)^2 p_{i-1,m}^{(2)}$$

$$- \frac{1}{2}\left(\frac{\Delta y}{\Delta x}\right)^2 p_{i+1,m}^{(2)} + 2\pi\eta\ \Delta y \left(\kappa_t\right)_{i,m} p_{i,m}^{(1)} = 0 \tag{49}$$

Similar equations exist at the lower boundary (see appendix D). The subscripts on σ and κ indicate that these quantities can vary along the length of the duct.

At the duct exit, the impedance condition

$$\kappa_e = 1 \tag{50}$$

$$\sigma_e = 0 \tag{51}$$

is used so that a finite duct can approximate a duct of infinite length (see appendixes B and E for detailed discussion). For this case, the finite difference approximations to equations (31) and (32) become at the exit ($i = n$)

$$p_{n,j}^{(1)}\left[1 + \left(\frac{\Delta x}{\Delta y}\right)^2 - \frac{(2\pi\eta\ \Delta x)^2}{2}\right] - p_{n-1,j}^{(1)} - \frac{1}{2}\left(\frac{\Delta x}{\Delta y}\right)^2 p_{n,j+1}^{(1)}$$

$$- \frac{1}{2}\left(\frac{\Delta x}{\Delta y}\right)^2 p_{n,j-1}^{(1)} - 2\pi\eta\ \Delta x p_{n,j}^{(2)} = 0 \qquad (52)$$

$$p_{n,j}^{(2)}\left[1 + \left(\frac{\Delta x}{\Delta y}\right)^2 - \frac{(2\pi\eta\ \Delta x)^2}{2}\right] - p_{n-1,j}^{(2)} - \frac{1}{2}\left(\frac{\Delta x}{\Delta y}\right)^2 p_{n,j+1}^{(2)}$$

$$- \frac{1}{2}\left(\frac{\Delta x}{\Delta y}\right)^2 p_{n,j-1}^{(2)} + 2\pi\eta\ \Delta x p_{n,j}^{(2)} = 0 \qquad (53)$$

Finally, special consideration must be given to the corners at the exit of the duct, $i = n$ and $j = m$, since both the exit and side wall impedance values influence this point. As a result, the impedance condition at the corner is

$$p_{n,m}^{(1)}\left[1 + \left(\frac{\Delta y}{\Delta x}\right)^2 + 2\pi\eta\ \Delta y\left(\sigma_t\right)_{n,m} - \frac{(2\pi\eta\ \Delta y)^2}{2}\right]$$

$$- \left(\frac{\Delta y}{\Delta x}\right)^2 p_{n-1,m}^{(1)} - p_{n,m-1}^{(1)} - 2\pi\eta\ \Delta y\left[\left(K_t\right)_{n,m} + \left(\frac{\Delta y}{\Delta x}\right)\right] p_{n,m}^{(2)} = 0 \qquad (54)$$

$$p_{n,m}^{(2)}\left[1 + \left(\frac{\Delta y}{\Delta x}\right)^2 + 2\pi\eta\ \Delta y\left(\sigma_t\right)_{n,m} - \frac{(2\pi\eta\ \Delta y)^2}{2}\right]$$

$$- \left(\frac{\Delta y}{\Delta x}\right)^2 p_{n-1,m}^{(2)} - p_{n,m-1}^{(2)} + 2\pi\eta\ \Delta y\left[\left(K_t\right)_{n,m} + \left(\frac{\Delta y}{\Delta x}\right)\right] p_{n,m}^{(1)} = 0 \qquad (55)$$

Axial Intensity

In terms of the difference notation, the axial intensity as given by equation (42) can be expressed as

$$I_{ij} = \frac{1}{2\pi\eta\,\Delta x}\left[p_{i,j}^{(2)}\left(p_{i,j}^{(1)} - p_{i-1,j}^{(1)}\right) - p_{i,j}^{(1)}\left(p_{i,j}^{(2)} - p_{i-1,j}^{(2)}\right)\right] \tag{56}$$

The total intensity across the test section, as given by equation (43) is written in difference notation as

$$E_i = \left[\frac{1}{2}I_{i,1} + \sum_{j=2}^{m-1} I_{i,j} + \frac{1}{2}I_{i,m}\right]\Delta y \tag{57}$$

We shall now apply the difference equations to the problem of noise attenuation in a duct.

MATRIX SOLUTION

The collection of the various difference equations at each grid point forms a set of simultaneous equations which can be expressed in matrix notation as

$$A \cdot \overline{P} = \overline{F} \tag{58}$$

where A is the coefficient matrix, $\overline{P}$ is the pressure matrix containing the unknown pressures, and $\overline{F}$ is the known matrix containing the various initial conditions, where A, $\overline{P}$, and $\overline{F}$ are complex in general.

In considering solutions to equation (58), it is convenient to express this equation in terms of all real quantities. To accomplish this, the matrix $\overline{P}$ is written as a column vector in terms of the $p^{(1)}$ and $p^{(2)}$ pressures and subdivided as follows:

$$\left[\begin{array}{c|c} A_1 & -C \\ \hline C & A_1 \end{array}\right] \left[\begin{array}{c} \overline{P}^{(1)} \\ \hline \overline{P}^{(2)} \end{array}\right] = \left[\begin{array}{c} \overline{F}^{(1)} \\ \hline \overline{F}^{(2)} \end{array}\right] \tag{59}$$

The upper left A_1 matrix is associated with the $p^{(1)}$ terms and the lower right A_1 matrix is associated with the $p^{(2)}$ terms. Both matrices are identical because of symmetry which exists in the governing equations. The A_1 matrix has a form typical of those matrices found in two-dimensional heat conduction problems or neutron diffusion problems. The A_1 matrix has one main diagonal element and four other diagonal ele-

ments which represent the coupling of the central point to the four adjacent points.

The C matrix represents the coupling that occurs between the $p^{(1)}$ and $p^{(2)}$ pressures through the impedance boundary conditions. The lower left matrix differs from the upper right matrix only by a change of sign. The C matrix is a sparse matrix with only one main diagonal term.

To better illustrate the detailed structure of the matrix given by equation (59), consider the simple example shown in figure 3. For this simple case the detailed matrix structure becomes

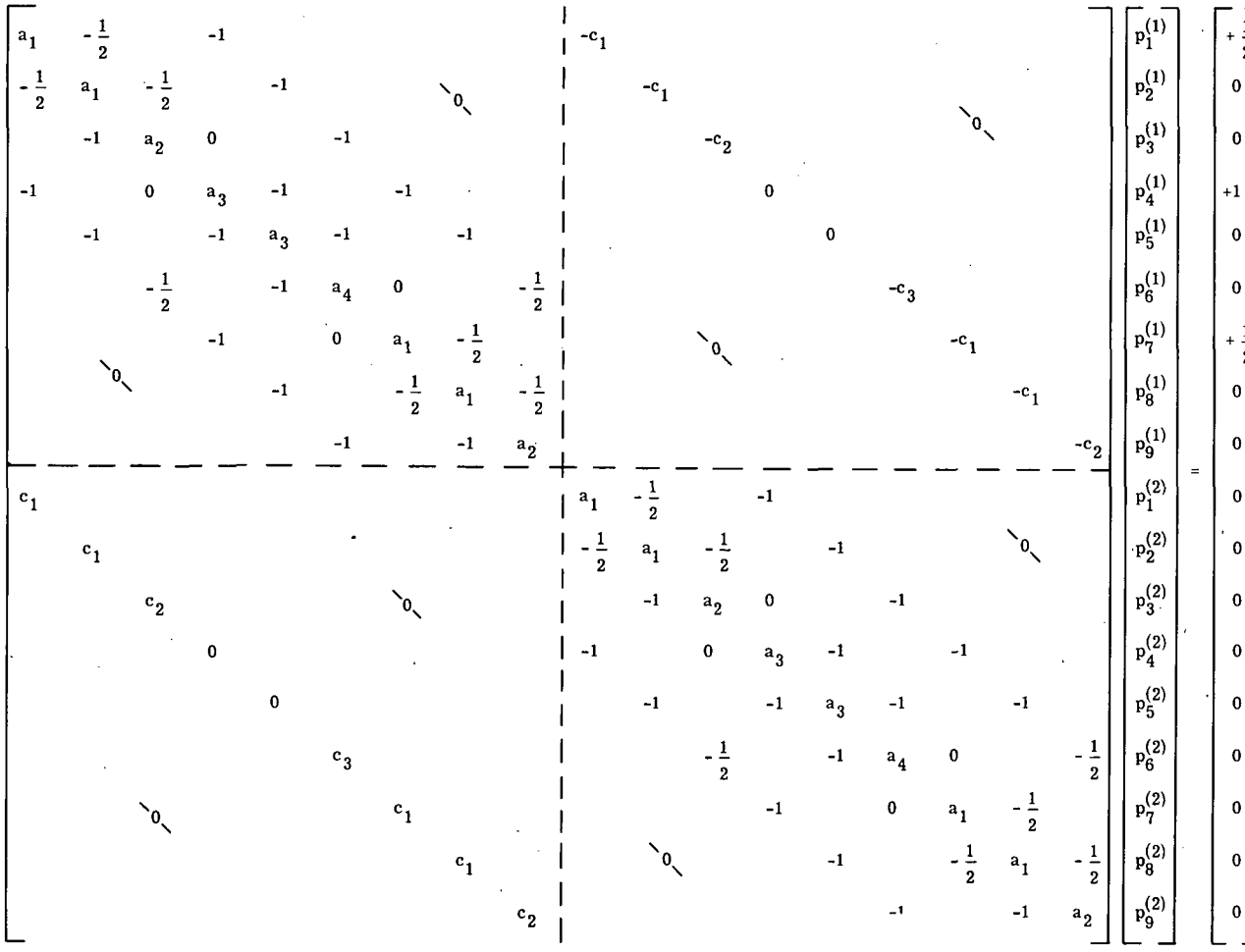

where the values of the coefficients a and c in this matrix are given in appendix D, along with the derivation of the other elements in this matrix equation.

As shown in appendix D, the constants a and c depend on the impedance and the grid size. The double-subscript notation, illustrated in figure 2, has now been replaced by a single-subscript notation. However, the double-subscript notation will still be used to set up the basic form of the matrix coefficients.

Matrices of the form of equation (59) can be solved by elimination techniques. In particular, the Gauss elimination technique was used to find a solution in the example problems which follow.

EXAMPLE PROBLEMS

Two examples are presented to illustrate the numerical technique. Both examples have analytical solutions; therefore, a direct comparison between the numerical and analytical techniques can be made. As mentioned in the INTRODUCTION, these examples are used to establish rules of thumb for choosing grid sizes for various frequencies and duct lengths. The first example presents a solution for a one-dimensional hard-wall duct with the impedance specified at the duct exit. The second example presents a solution for the propagation of sound in a two-dimensional straight soft-wall duct.

Example 1 - One-Dimensional Hard-Wall Duct of Infinite Length

As our first example of the difference technique, we shall consider the problem of an infinite hard-wall duct with a plane pressure wave at the entrance of the duct.

In this case, "hard wall" implies that

$$Z_t = \infty \qquad y = 0 \qquad \text{and} \quad y = 1 \tag{61}$$

or

$$\kappa_t = 0 \qquad y = 0 \qquad \text{and} \quad y = 1 \tag{62}$$

$$\sigma_t = 0 \qquad y = 0 \qquad \text{and} \quad y = 1 \tag{63}$$

For this special case of a plane wave entrance condition, no pressure gradients will exit in the transverse direction in the duct; consequently, the Helmholtz representation of the wave equation, equation (11), reduces to the one-dimensional form

$$\frac{\partial^2 p}{\partial x^2} + (2\pi\eta)^2 p = 0 \tag{64}$$

The difference form of the general equation presented earlier can be simplified by noting that

$$\ldots = p^{(\ )}_{i,j-1} = p^{(\ )}_{i,j} = p^{(\ )}_{i,j+1} = p^{(\ )}_{i,j+2} = \ldots \tag{65}$$

In this case, the difference form of the wave equation, equation (45), reduces to

$$-p^{(1)}_{i-1,j} - p^{(1)}_{i+1,j} + \left[2 - (2\pi\eta\ \Delta x)^2\right] p^{(1)}_{i,j} = 0 \tag{66}$$

with an identical expression for $p^{(2)}$ component of pressure.

The word "infinite" used in the title of this example problem implies that the duct is sufficiently long so that no reflective waves occur in the duct. In the numerical formulation of the infinite duct, we can simulate the infinite duct by assuming a finite length of duct and applying an impedance of value ρc at the exit plane of the duct (see appendix B for proof). As a result, $\kappa_e = 1$ (eq. (B12)) and $\sigma_e = 0$. Thus, the exit impedance boundary conditions corresponding to equations (52) and (53) become

$$p^{(1)}_{n,j}\left[1 - \frac{(2\pi\eta\ \Delta x)^2}{2}\right] - p^{(1)}_{n-1,j} - 2\pi\eta\ \Delta x p^{(2)}_{n,j} = 0 \tag{67}$$

$$p^{(2)}_{n,j}\left[1 - \frac{(2\pi\eta\ \Delta x)^2}{2}\right] - p^{(2)}_{n-1,j} + 2\pi\eta\ \Delta x p^{(2)}_{n,j} = 0 \tag{68}$$

The entrance conditions are simply

$$p^{(1)}(0) = 1 \tag{69}$$

$$p^{(2)}(0) = 0 \tag{70}$$

In solving the resulting set of matrix equations we will simplify the structure of the solution matrix. This simplification should be useful in future work if block iteration techniques (ref. 18) are applied to the solution of the two-dimensional matrix equations.

Consider the simple case shown in figure 4, where four points are used to describe the pressure distribution in a finite hard-wall duct with ρc exit impedance. In this case, the general matrix equation, equation (59), reduces to the following form:

$$
\begin{bmatrix}
a_1 & -1 & & & 0 & & & \\
-1 & a_1 & -1 & & & 0 & & \\
 & -1 & a_1 & -1 & & & 0 & \\
 & & -1 & a_2 & & & & -c_1 \\
0 & & & & a_1 & -1 & & \\
 & 0 & & & -1 & a_1 & -1 & \\
 & & 0 & & & -1 & a_1 & -1 \\
 & & & c_1 & & & -1 & a_2
\end{bmatrix}
\times
\begin{bmatrix} p_1^{(1)} \\ p_2^{(1)} \\ p_3^{(1)} \\ p_4^{(1)} \\ p_1^{(2)} \\ p_2^{(2)} \\ p_3^{(2)} \\ p_4^{(2)} \end{bmatrix}
=
\begin{bmatrix} 1 \\ 0 \\ 0 \\ 0 \\ 0 \\ 0 \\ 0 \\ 0 \end{bmatrix}
\qquad (71)
$$

where

$$a_1 = 2 - (2\pi\eta\ \Delta x)^2$$

$$a_2 = 1 - \frac{(2\pi\eta\ \Delta x)^2}{2}$$

$$c_1 = 2\pi\eta\ \Delta x$$

As seen in equation (71), the basic structure of the solution matrix is similar to the structure shown in equation (60). The A_1 matrices become tridiagonal and the coupling C matrix has only one element.

The detailed structure of equations (60) and (71) are arbitrary, since we are free to construct the column vector $\overline{P}$ in a variety of ways. Therefore, for one-dimensional problems, we shall now redefine the column vector $\overline{P}$ to be of the form

$$\overline{P} = \begin{bmatrix} p_1^{(1)} \\ p_2^{(1)} \\ \cdot \\ \cdot \\ \cdot \\ p_{n-1}^{(1)} \\ p_n^{(1)} \\ p_n^{(2)} \\ p_{n-1}^{(2)} \\ \cdot \\ \cdot \\ \cdot \\ p_2^{(2)} \\ p_1^{(2)} \end{bmatrix} \tag{72}$$

where the $p^{(2)}$ components have been inverted. For the special case of $n = 4$, as shown in figure 4,

$$\overline{P} = \begin{bmatrix} p_1^{(1)} \\ p_2^{(1)} \\ p_3^{(1)} \\ p_4^{(1)} \\ p_4^{(2)} \\ p_3^{(2)} \\ p_2^{(2)} \\ p_1^{(2)} \end{bmatrix} \tag{73}$$

Expressing the general matrix equation (58) in terms of this new column vector gives for our simple example the following matrix equation:

$$\left[\begin{array}{cccc|cccccccc} a_1 & -1 & & & & & & & & & & \\ -1 & a_1 & -1 & & & & & & & & & \\ & -1 & a_1 & -1 & & & & 0 & & & & \\ & & -1 & a_2 & -c & & & & & & & \\ \hline & & & c & a_2 & -1 & & & & & & \\ & & & & -1 & a_1 & -1 & & & & & \\ & & 0 & & & -1 & a_1 & -1 & & & & \\ & & & & & & -1 & a_1 & & & & \end{array}\right] \times \begin{bmatrix} p_1^{(1)} \\ p_2^{(1)} \\ p_3^{(1)} \\ p_4^{(1)} \\ p_4^{(2)} \\ p_3^{(2)} \\ p_2^{(2)} \\ p_1^{(2)} \end{bmatrix} = \begin{bmatrix} 1 \\ 0 \\ 0 \\ 0 \\ 0 \\ 0 \\ 0 \\ 0 \end{bmatrix}$$

where a_1, a_2, and c are the same as defined in equation (71). As seen in equation (74), the resulting coefficient matrix is tridiagonal, which is extremely easy to solve.

Equation (74) was applied to a duct with a height-length ratio L/H of 1 and a dimensionless frequency η of 1. For a value of $n = 12$, the numerical as well as the analytical results are shown in figure 5. As seen in figure 5, the numerical and analytical results are in good agreement.

In determining the attenuation of a particular liner, we are interested in how well the difference formulation predicts the intensity at the duct exit. Figure 6 displays the numerical results for axial intensity at the duct exit for a variety of dimensionless frequencies η. Recall that the intensity was nondimensionalized such that it is identical to 1 for a hard-wall duct. For a sparse number of grid points n, the numerical results fall below the analytical value of 1. However, as the number of grid points is increased, the numerical value of the intensity asymptotically approaches the theoretical value of 1.

From the numerical results shown in figure 6, we can establish the following rule of thumb for one-dimensional problems:

$$n = 12\eta \frac{L}{H} = 12 \frac{L}{\lambda} \quad \text{for } Z_t = \infty,\ Z_e = \rho c \tag{75}$$

or

$$\Delta x = \frac{\lambda}{12} \quad \text{for} \quad Z_t = \infty, \; Z_e = \rho c \tag{76}$$

That is, for a given L/H or η, if we choose n greater than or equal to the value suggested by equation (75), the calculated value of I will be within 4 percent of the true value.

For the two-dimensional problem with finite Z_t, equation (75) will not hold. Because the intensity can vary inside the duct in the transverse direction in the two-dimensional problems, more grid points will be necessary to assess the intensity in two-dimensional problems. Consequently, for the general two-dimensional case

$$n > 12\eta \frac{L}{H} \quad \text{for} \quad Z_t < \infty, \; Z_e = \rho c \tag{77}$$

Example 2 - Propagation of Sound in a Two-Dimensional Soft-Wall Duct

In our second example of the difference technique, we shall consider the problem of calculating the maximum attenuation possible in a two-dimensional duct with L/H of 0.5 and dimensionless frequencies η of 0.6 and 1. We can compare the numerical results to the analytical results found by using the techniques presented by Rice (ref. 4).

The first step in determining the maximum attenuation in the duct is to calculate the attenuation at various Z-values in the impedance plane. This is shown in figure 7, where

$$\zeta = \frac{Z}{\rho c} = \theta + i\chi \tag{78}$$

defines the impedance plane. As seen in figure 7, the peak occurs at negative values of wall reactance. The sound attenuation values shown in figure 7 were obtained by choosing discrete values of θ and χ throughout the θ-χ plane, calculating the sound attenuation at each point, and interpolating between the points to obtain smooth contours. The impedance associated with the peak attenuation is called the optimum impedance.

As was previously mentioned in this report, the solution matrix for the acoustic flow field is not positive definite; consequently, conventional iteration techniques cannot be used to solve the difference equations. This is a serious limitation, since iteration techniques generally are quicker and require a much smaller storage in the computer than conventional elimination procedures. Nevertheless, a standard elimination subprogram was used.

Because of matrix-size limitations in the elimination subprogram used to solve equation (59), the technique of varying grid size (ref. 19) was used. This technique is illustrated in figure 8, where the grid spacing Δy is decreased toward zero. The attenuation at the optimum impedance is found by extrapolating the grid size to zero (dashed portion of the curve). As shown in figure 8, the extrapolated numerical values are in agreement with the analytical values calculated from the theory presented by Rice in reference 4.

Based on the known computational times for the solutions presented in this report, we can now estimate the computer time involved in solving some realistic liner problems. We will assume that an elimination subprogram will be available which is specially tailored to the particular acoustic matrix; that is, no zero need be stored in the subprogram. Furthermore, we will assume that 1000 grid points will adequately describe the liner geometry to be analyzed. For the two-dimensional example problem considered in this report, the solution would require approximately 0.4 minute of computer time. In the future, when nonuniform shear flow effects are incorporated into the governing flow equations, the computer time will increase by a factor of 3, to 1.2 minutes. Both time estimates are quite acceptable for liner design calculations.

The numerical procedure is quite flexible and can be used to obtain details of the acoustic field structure, such as pressure, velocity, and intensity, at any position in the duct. Complications such as variable impedance or wall geometry are easily programmed.

CONCLUDING REMARKS

Finite difference solutions are presented for sound propagation in a one-dimensional hard-wall duct and a two-dimensional soft-wall duct for zero Mach number. The results show the numerical procedure to be in agreement with the corresponding exact analytical results. Because the solution matrix for the acoustic flow field is not positive definite, conventional iteration techniques cannot be used to solve the difference equations. Before the finite difference formulation can be applied to more complicated problems which require a large number of grid points, such as the sonic inlet, iteration techniques will have to be developed to overcome present grid-size limitations.

The finite difference formulation is flexible and should be a powerful tool in the solution of more realistic studies of inlet and exhaust ducts of turbofan engines. The present formulation allows complete freedom in choosing the inlet pressure profile and

the complex impedance along both boundaries. The extension of the present formulation to both uniform flow and shear flow is straightforward.

Lewis Research Center,
National Aeronautics and Space Administration,
Cleveland, Ohio, April 10, 1973,
501-04.

APPENDIX A

SYMBOLS

A	coefficient matrix, eq. (58)
A_1	submatrix, eq. (59)
a_1, a_2, a_3, a_4	elements of matrix A_1
C	submatrix, eq. (59)
c	speed of sound
c_1, c_2, c_3	elements of matrix C
ΔdB	decrease in decibels, eq. (44)
E	acoustic power, eq. (43)
$\overline{F}$	matrix, eq. (58)
f	frequency
$f(K_j)$	function of K_j
$f(y)$	function of y
$G(y)$	arbitrary function of y
H	channel height, fig. 1
I	dimensionless acoustic intensity, eq. (41)
I'	dimensional acoustic intensity, eq. (39)
i	$\sqrt{-1}$
K_j	complex propagation constant
k	wave number, ω/c
L	dimensional length of duct
m	total number of grid rows (points in y-direction)
n	total number of grid columns (points in x-direction)
O	order of
$\overline{P}$	pressure column vector, eq. (58)
P'	dimensional pressure, $P'(x',y',t)$
p	dimensionless pressure fluctuation, eq. (10)

p_A	amplitude of pressure fluctuation at duct entrance
p'	dimensional pressure fluctuation
t	time
$\bar{u}$	dimensionless acoustic particle velocity, eq. (22)
$\bar{u}'$	dimensional acoustic particle velocity
x	dimensionless axial coordinate, eq. (9)
Δx	axial grid spacing
x'	dimensional axial coordinate, fig. 1
y	dimensionless transverse coordinate, eq. (8)
Δy	transverse grid spacing
y'	dimensional transverse coordinate, fig. 1
Z	acoustic impedance
ζ	dimensionless specific acoustic impedance
η	dimensionless frequency, eq. (12)
κ	acoustic conductance ratio
λ	wavelength
ρ	density
σ	acoustic susceptance ratio
θ	dimensionless specific acoustic resistance
χ	dimensionless specific acoustic reactance
ω	circular frequency

Operators:

∇^2	Laplacian
∇	gradient

Subscripts:

e	exit condition
i, j	axial and transverse indexes, respectively, fig. 2
j	mode index
t	transverse y-direction

x	axial position
y	transverse position

Superscripts:

'	dimensional quantity
*	complex conjugate
($\bar{}$)	vector quantity
(1)	real part
(2)	imaginary part

APPENDIX B

ONE-DIMENSIONAL SOUND PROPAGATION IN AN INFINITE DUCT

Pressure Field

For one-dimensional sound propagation in the x-direction, the dimensionless wave equation, equation (11), reduces to

$$\frac{d^2p}{dx^2} + (2\pi\eta)^2 p = 0 \tag{B1}$$

In this case, the waves are uniform with no gradients in the y-direction. The general solution of equation (B1) is

$$p = Ae^{-i2\pi\eta x} + Be^{+i2\pi\eta x} \tag{B2}$$

The boundary conditions for equation (B2) are as follows

$$B = 0 \quad \text{(no reflecting waves)} \tag{B3}$$

$$p = 1 \quad \text{at } x = 0 \tag{B4}$$

Applying conditions (B3) and (B4) to equation (B2) gives as a solution

$$p = e^{-i2\pi\eta x} \tag{B5}$$

or

$$p = \cos 2\pi\eta x - i \sin 2\pi\eta x \tag{B6}$$

Thus, in terms of the real and imaginary pressures in the numerical solutions

$$p^{(1)} = \cos 2\pi\eta x \tag{B7}$$

$$p^{(2)} = -\sin 2\pi\eta x \tag{B8}$$

Terminal Impedance

The specific acoustic impedance ζ at any point is defined by equation (25) and is given for the x-direction as

$$\zeta_x = -i2\pi\eta \left.\frac{p}{\frac{\partial p}{\partial x}}\right)_x \tag{B9}$$

Substituting equation (B5) into equation (B9) gives the impedance at any position x as

$$\zeta_x = 1 \tag{B10}$$

or the impedance at any position from equation (24) as

$$Z = \rho c \tag{B11}$$

In terms of the acoustic conductance and susceptance ratios, defined by equation (27),

$$\kappa = 1 \tag{B12}$$

$$\sigma = 0 \tag{B13}$$

These results can be used in the numerical analysis to allow a finite length of duct to represent an infinite duct by using $\kappa_e = 1$ and $\sigma_e = 0$.

Intensity

The dimensionless axial acoustic intensity is given in the body of this report as

$$I = \frac{1}{2\pi\eta}\left[p^{(2)}\ \frac{\partial p^{(1)}}{\partial x} - p^{(1)}\ \frac{\partial p^{(2)}}{\partial x}\right] \tag{42}$$

Substituting equations (B7) and (B8) into equation (42) and collecting terms gives

$$I = 1 \tag{B14}$$

Thus, the axial acoustical intensity is invariant along the length of the duct.

APPENDIX C

FINITE DIFFERENCE EQUATIONS

The basic difference equations are determined by integrating the appropriate differential equation over a unit cell, as shown in figure 9. The cell is enclosed by the dashed lines which are spaced midway between the grid lines (not shown). The grid lines would go directly through the grid points. In this particular problem, the governing equation is the wave equation as given by equation (14) or (15) in the body of the report. Thus, the finite difference integrals become

$$\iint_{\text{cell}} \left[\nabla^2 p^{(1)} + (2\pi\eta)^2 p^{(1)}\right] dA = 0 \tag{C1}$$

$$\iint_{\text{cell}} \left[\nabla^2 p^{(2)} + (2\pi\eta)^2 p^{(2)}\right] dA = 0 \tag{C2}$$

By applying Green's theorem for the plane region, these equations reduce to

$$\oint_{\text{cell}} \frac{\partial p^{(1)}}{\partial n}\, ds + (2\pi\eta)^2 \iint_{\text{cell}} p^{(1)}\, dA = 0 \tag{C3}$$

$$\oint_{\text{cell}} \frac{\partial p^{(2)}}{\partial n}\, ds + (2\pi\eta)^2 \iint_{\text{cell}} p^{(2)}\, dA = 0 \tag{C4}$$

where dA is a differential area element of the unit cell, ds is the differential length on the boundary of the unit cell, and n is the normal to the cell boundary.

As usual, the difference formulation approximates the first derivatives as follows:

$$\left.\frac{\partial p}{\partial x}\right|_{i+\frac{1}{2},\, j} = \frac{p_{i+1,\,j} - p_{i,\,j}}{\Delta x} + O\left[\Delta x^2\right]$$

$$\left.\frac{\partial p}{\partial y}\right|_{i,\,j+\frac{1}{2}} = \frac{p_{i,\,j+1} - p_{i,\,j}}{\Delta y} + O\left[\Delta y^2\right]$$

Wave Equation

The wave equation in finite difference form, equation (47) in the body of the report, is developed by applying equation (C3) to the cell marked 1 in figure 9. In evaluating the surface integrals, the gradients are assumed to be constant on each side of the cell and the interior pressure is assumed to be constant in the interior of the cell. Thus, equation (C3) becomes

$$\frac{p^{(1)}_{i-1,\,j} - p^{(1)}_{i,\,j}}{\Delta x}\,\Delta y + \frac{p^{(1)}_{i,\,j-1} - p^{(1)}_{i,\,j}}{\Delta y}\,\Delta x + \frac{p^{(1)}_{i+1,\,j} - p_{i,\,j}}{\Delta x}\,\Delta y + \frac{p^{(1)}_{i,\,j+1} - p^{(1)}_{i,\,j}}{\Delta y}\,\Delta x + (2\pi\eta)^2 p^{(1)}_{i,\,j}\,\Delta x\,\Delta y = 0 \qquad \text{(C5)}$$

Multiplying all terms by $-\Delta x/\Delta y$ and collecting terms gives

$$-p^{(1)}_{i-1,\,j} - p^{(1)}_{i+1,\,j} - \left(\frac{\Delta x}{\Delta y}\right)^2\left[p^{(1)}_{i,\,j-1} + p^{(1)}_{i,\,j+1}\right] + \left[2 + 2\left(\frac{\Delta x}{\Delta y}\right)^2 - (2\pi\eta\,\Delta x)^2\right] p^{(1)}_{i,\,j} = 0 \qquad \text{(C6)}$$

which is equation (45) in the body of the report. Using the same procedure, the difference equation for the $p^{(2)}$ component can also be found.

Finally, let us consider the difference equation which applies in cell 2, which is adjacent to the upper boundary in figure 9. For this unit cell, equation (C3) can be expressed as

$$\frac{p^{(1)}_{i-1,m} - p^{(1)}_{i,m}}{\Delta x}\,\frac{\Delta y}{2} + \frac{p^{(1)}_{i,m-1} - p^{(1)}_{i,m}}{\Delta y}\,\Delta x + \frac{p^{(1)}_{i+1,m} - p^{(1)}_{i,m}}{\Delta x}\,\frac{\Delta y}{2}$$

$$+ \left.\frac{\partial p^{(1)}}{\partial n}\right|_{\substack{\text{wall}\\ y=1}} \Delta x + (2\pi\eta)^2 p^{(1)}_{i,m}\,\Delta x\,\frac{\Delta y}{2} = 0 \qquad \text{(C7)}$$

The normal derivative at the wall, $\partial p/\partial y$ is given by the known impedance boundary condition given by equation (29) in the body of the report, which is repeated here for convenience

$$\frac{\partial p^{(1)}}{\partial y} = -2\pi\eta\left[p^{(1)}\sigma_t - p^{(2)}\kappa_t\right] \qquad (29)$$

In difference form,

$$\left.\frac{\partial p^{(1)}}{\partial y}\right|_{y=1} = -2\pi\eta\left[p^{(1)}_{i,m}\left(\sigma_t\right)_{i,m} - p^{(2)}_{i,m}\left(\kappa_t\right)_{i,m}\right] \qquad \text{(C8)}$$

Substituting equation (C8) into equation (C7) and collecting terms yields

$$p^{(1)}_{i,m}\left[1 + \left(\frac{\Delta y}{\Delta x}\right)^2 + 2\pi\eta\,\Delta y\left(\sigma_t\right)_{i,m} - \frac{(2\pi\eta\,\Delta y)^2}{2}\right] - p^{(1)}_{i,m-1} - \frac{1}{2}\left(\frac{\Delta y}{\Delta x}\right)^2 p^{(1)}_{i-1,m}$$

$$- \frac{1}{2}\left(\frac{\Delta y}{\Delta x}\right)^2 p^{(1)}_{i+1,m} - 2\pi\eta\,\Delta y\left(\kappa_t\right)_{i,m} p^{(2)}_{i,n} = 0 \qquad \text{(C9)}$$

In a similar manner, equations (C3) and (C4) are applied to cells 2, 3, and 4 to yield equations (50) to (56) in the body of this report.

APPENDIX D

APPLICATION OF DIFFERENCE EQUATIONS TO SOFT-WALL DUCT

In this appendix, we develop some of the matrix coefficients which make up the matrix given by equation (60) in the body of this report. This matrix results from the difference formulation for sound propagation in a straight soft-wall duct for zero Mach number.

General Difference Equations at Lower Wall

Before looking at the specific form of equation (60), we will write the general form of the difference equations at the lower wall, since the coefficients in the first two rows of equation (60) result from applying the difference equations to points 1 and 2 along the lower wall shown in figure 3. At the lower wall, equations (48) and (49) can be written as

$$p_{i,1}^{(1)}\left[1 + \left(\frac{\Delta y}{\Delta x}\right)^2 + 2\pi\eta\ \Delta y\left(\sigma_t\right)_{i,1} - \frac{(2\pi\eta\ \Delta y)^2}{2}\right] - p_{i,2}^{(1)} - \frac{1}{2}\left(\frac{\Delta y}{\Delta x}\right)^2 p_{i-1,1}^{(1)}$$

$$- \frac{1}{2}\left(\frac{\Delta y}{\Delta x}\right)^2 p_{i+1,1}^{(1)} - 2\pi\eta\ \Delta y\left(\kappa_t\right)_{i,1} p_{i,1}^{(2)} = 0 \qquad \text{(D1)}$$

$$p_{i,1}^{(2)}\left[1 + \left(\frac{\Delta y}{\Delta x}\right)^2 + 2\pi\eta\ \Delta y\left(\sigma_t\right)_{i,1} - \frac{(2\pi\eta\ \Delta y)^2}{2}\right] - p_{i,2}^{(2)} - \frac{1}{2}\left(\frac{\Delta y}{\Delta x}\right)^2 p_{i-1,1}^{(2)}$$

$$- \frac{1}{2}\left(\frac{\Delta y}{\Delta x}\right)^2 p_{i+1,1}^{(2)} + 2\pi\eta\ \Delta y\left(\kappa_t\right)_{i,1} p_{i,1}^{(1)} = 0 \qquad \text{(D2)}$$

In this example, $\Delta y = \Delta x$; therefore, the ratio $\Delta x/\Delta y = 1$; thus, these equations reduce to

$$p_{i,1}^{(1)}\left[2 + 2\pi\eta\ \Delta y\left(\sigma_t\right)_{i,1} - \frac{(2\pi\eta\ \Delta y)^2}{2}\right] - p_{i,2}^{(1)} - \frac{1}{2}\left[p_{i-1,1}^{(1)} + p_{i+1,1}^{(1)}\right]$$

$$- 2\pi\eta\ \Delta y\left(\kappa_t\right)_{i,1} p_{i,1}^{(2)} = 0 \tag{D3}$$

$$p_{i,1}^{(2)}\left[2 + 2\pi\eta\ \Delta y\left(\sigma_t\right)_{i,1} - \frac{(2\pi\eta\ \Delta y)^2}{2}\right] - p_{i,2}^{(2)} - \frac{1}{2}\left[p_{i-1,1}^{(2)} + p_{i+1,1}^{(2)}\right]$$

$$+ 2\pi\eta\ \Delta y\left(\kappa_t\right)_{i,1} p_{i,1}^{(1)} = 0 \tag{D4}$$

For simplicity, we now define

$$a_1 = 2 + 2\pi\eta\ \Delta y\left(\sigma_t\right)_{i,1} - \frac{(2\pi\eta\ \Delta y)^2}{2} \tag{D5}$$

and

$$c_1 = 2\pi\eta\ \Delta y\left(\kappa_t\right)_{i,1} \tag{D6}$$

Substituting equations (D5) and (D6) into equations (D3) and (D4) yields

$$a_1 p_{i,1}^{(1)} - p_{i,2}^{(1)} - \frac{1}{2}\left[p_{i-1,1}^{(1)} + p_{i+1,1}^{(1)}\right] - c_1 p_{i,1}^{(2)} = 0 \tag{D7}$$

$$a_1 p_{i,1}^{(2)} - p_{i,2}^{(2)} - \frac{1}{2}\left[p_{i-1,1}^{(2)} + p_{i+1,1}^{(2)}\right] + c_1 p_{i,1}^{(1)} = 0 \tag{D8}$$

In a similar manner, the difference equations at the lower corner take on the form

$$a_2 p_{n,1}^{(1)} - p_{n-1,1}^{(1)} - p_{n,2}^{(1)} - c_2 p_{n,1}^{(2)} = 0 \tag{D9}$$

$$a_2 p_{n,1}^{(2)} - p_{n-1,1}^{(2)} - p_{n,2}^{(2)} + c_2 p_{n,1}^{(1)} = 0 \tag{D10}$$

where

$$a_2 = 2 + 2\pi\eta\ \Delta y\left(\sigma_t\right)_{n,1} - \frac{(2\pi\eta\ \Delta y)^2}{2} \tag{D11}$$

$$c_2 = 2\pi\eta\ \Delta y\left[1 + \left(\kappa_t\right)_{n,1}\right] \tag{D12}$$

Application to Equation (60)

We shall now apply these equations and the other equations derived elsewhere in this report to the derivation of equation (60).

Point 1. - The double-subscript notation will be transformed into the single-subscript notation used in figure 3 for this example. Applying equation (D7) to point 1 yields

$$a_1 p_1^{(1)} - p_4^{(1)} - \frac{1}{2}\left[p_0^{(1)} + p_2^{(1)}\right] - c_1 p_1^{(2)} = 0 \tag{D13}$$

where a_1 and c_1 are defined by equations (D5) and (D6). However, p_0 represents an initial-condition grid point, which in this example has a value of 1. Thus, equation (D13) becomes

$$a_1 p_1^{(1)} - \frac{1}{2} p_2^{(1)} - p_4^{(1)} - c_1 p_1^{(2)} = \frac{1}{2} \tag{D14}$$

or in matrix form

$$\left(a_1 \; -\frac{1}{2} \; 0 \; -1 \; 0 \; 0 \; 0 \; 0 \; 0 \; -c_1 \; 0 \; 0 \; 0 \; 0 \; 0 \; 0 \; 0 \; 0 \; 0\right) \times \begin{pmatrix} p_1^{(1)} \\ p_2^{(1)} \\ p_3^{(1)} \\ p_4^{(1)} \\ p_5^{(1)} \\ p_6^{(1)} \\ p_7^{(1)} \\ p_8^{(1)} \\ p_9^{(1)} \\ p_1^{(2)} \\ p_2^{(2)} \\ \vdots \\ p_9^{(2)} \end{pmatrix} = \begin{pmatrix} \frac{1}{2} \end{pmatrix} \tag{D15}$$

which represents the first row in equation (60).

The imaginary $p^{(2)}$ pressure equation at point 1 results from applying equation (D8) to point 1. This yields

$$a_1 p_1^{(2)} - p_4^{(2)} - \frac{1}{2}\left[p_0^{(2)} + p_2^{(2)}\right] + c_1 p_1^{(1)} = 0 \tag{D16}$$

In this case, however, $p_0^{(2)}$ represents a zero initial condition; thus, equation (D16) becomes

$$c_1 p_1^{(1)} + a_1 p_1^{(2)} - \frac{1}{2} p_2^{(2)} - p_4^{(2)} = 0 \tag{D17}$$

which represents the 10th row of equation (60). The matrix form of equation (D17) is similar to equation (D15).

Point 2. - At point 2, equations (D7) and (D8) become

$$-\frac{1}{2}p_1^{(1)} + a_1 p_2^{(1)} - \frac{1}{2}p_3^{(1)} - p_5^{(1)} - c_1 p_2^{(2)} = 0 \tag{D18}$$

and

$$-\frac{1}{2}p_1^{(2)} + a_1 p_2^{(2)} - \frac{1}{2}p_3^{(2)} - p_5^{(2)} + c_1 p_2^{(1)} = 0 \tag{D19}$$

which represents the second and 11th rows of equation (60).

Point 3. - At point 3, equations (D9) and (D10) become

$$-p_2^{(1)} + a_2 p_3^{(1)} - p_6^{(1)} - c_2 p_3^{(2)} = 0 \tag{D20}$$

and

$$-p_2^{(2)} + a_2 p_3^{(2)} - p_6^{(2)} + c_2 p_3^{(1)} = 0 \tag{D21}$$

which represent the third and 12th rows of equation (60).

Point 4. - At point 4, equations (45) and (46) in the body of this report become

$$-p_0^{(1)} - p_5^{(1)} - p_1^{(1)} - p_7^{(1)} + \left[4 - (2\pi\eta\,\Delta x)^2\right]p_4^{(1)} = 0 \tag{D22}$$

and

$$-p_0^{(2)} - p_5^{(2)} - p_1^{(2)} - p_7^{(2)} + \left[4 - (2\pi\eta\,\Delta x)^2\right]p_4^{(2)} = 0 \tag{D23}$$

But from the initial condition, $p_0^{(1)} = 1$ while $p_0^{(2)} = 0$; thus equations (D22) and (D23) become

$$-p_1^{(1)} + a_3 p_4^{(1)} - p_5^{(1)} - p_7^{(1)} = 1 \tag{D24}$$

$$-p_1^{(2)} + a_3 p_4^{(2)} - p_5^{(2)} - p_7^{(2)} = 0 \tag{D25}$$

where

$$a_3 = 4 - (2\pi\eta\ \Delta x)^2 \tag{D26}$$

Equations (D24) and (D25) represent the fourth and 13th lines in equation (60).

Point 5. - The difference equations that apply at point 5 come directly from equations (45) and (46) as

$$-p_2^{(1)} - p_4^{(1)} + a_3 p_5^{(1)} - p_6^{(1)} - p_8^{(1)} = 0 \tag{D27}$$

and

$$-p_2^{(2)} - p_4^{(2)} + a_3 p_5^{(2)} - p_6^{(2)} - p_8^{(2)} = 0 \tag{D28}$$

These equations represent the fifth and 14th lines in equation (60). In an actual acoustic problem, the bulk of the difference equations in the central flow field will be of this form.

Point 6. - At point 6, equations (52) and (53) in the body of this report become

$$-\frac{1}{2} p_3^{(1)} - p_5^{(1)} + a_4 p_6^{(1)} - \frac{1}{2} p_9^{(1)} - c_3 p_6^{(2)} = 0 \tag{D29}$$

and

$$-\frac{1}{2} p_3^{(2)} - p_5^{(2)} + a_4 p_6^{(2)} - \frac{1}{2} p_9^{(2)} + c_3 p_6^{(1)} = 0 \tag{D30}$$

where

$$a_4 = 2 - \frac{(2\pi\eta\ \Delta x)^2}{2} \tag{D31}$$

and

$$c_3 = 2\pi\eta\ \Delta x \tag{D32}$$

Equations (D29) and (D30) represent the sixth and 15th lines in equation (60).

The equations for points 7, 8, and 9 are similar to the equations at points 1, 2, and 3. These equations will not be presented here.

APPENDIX E

CLOSURE PROBLEM

The close agreement between the numerical theory and the corresponding exact analytical results substantiates the utility of the ρc exit impedance assumption made earlier in this report. However, we shall now establish criteria for which the numerical and analytical results will be in exact agreement. To accomplish this task, we must first look at the analytical theory.

The analytical solution (ref. 7, e.g.) assumes that the solutions to the wave equation are separable and can be expressed in terms of an infinite number of modes. For only forward-going waves (no reflections, i.e., an infinite duct) the expressions for pressure and velocity are of the form

$$p,\ u_x,\ u_y \propto \sum_{j=1}^{N} G_j(y) e^{-ikK_j x} \tag{E1}$$

where K_j is a complex propagation coefficient for each mode.

The propagation constants K_j are functions of an eigenvalue μ_j. The eigenvalues μ_j are determined by the wall impedance condition

$$\zeta_t = 2\pi\eta \left.\frac{p_j}{u_{yj}}\right)_w \tag{E2}$$

A solution to equation (E2) yields an infinite set of eigenvalues μ_j, each identifiable with a mode. Also, as a direct consequence of equation (E2), it follows that for each mode

$$\left.\frac{p_1}{u_{y1}}\right)_w = \left.\frac{p_2}{u_{y2}}\right)_w = \left.\frac{p_3}{u_{y3}}\right)_w = \ldots = \left.\frac{p_j}{u_{yj}}\right)_w = \ldots \tag{E3}$$

Conversely, it follows that at some finite distance L down the infinite duct, which we label e for exit plane, the ratio of pressure to axial velocity is different for each mode:

$$\left.\frac{p_1}{u_{x1}}\right)_e \neq \left.\frac{p_2}{u_{x2}}\right)_e \neq \left.\frac{p_3}{u_{x3}}\right)_e \neq \ldots \neq \left.\frac{p_j}{u_{xj}}\right)_e \neq \ldots \tag{E4}$$

Equation (E4) follows as a consequence of the fact that this ratio depends on the eigenvalues (through K_j) which were previously determined by equation (E2):

$$\left.\frac{p_j}{u_{xj}}\right)_e = f(K_j) \tag{E5}$$

Thus, each ratio of pressure to axial velocity at the exit position takes on its own unique value depending on the values of the propagation constant K_j.

If we now define the axial impedance in the usual manner, the impedance condition for no reflection at $x = L$ becomes

$$\zeta_{e1} = 2\pi\eta \frac{p_1}{u_{x1}}, \quad \zeta_{e2} = 2\pi\eta \frac{p_2}{u_{x2}}, \quad \ldots, \quad \zeta_{ej} = 2\pi\eta \frac{p_j}{u_{xj}}, \quad \ldots \tag{E6}$$

That is, the infinite duct with no reflections could now be replaced by a finite duct of length L with each mode having its own respective exit impedance as given in equation (E6). Clearly, as a consequence of equations (E5) and (E6), the exit impedance conditions for no reflection are such that

$$\zeta_{e1} \neq \zeta_{e2} \neq \zeta_{e3} \neq \ldots \neq \zeta_{ej} \neq \ldots \tag{E7}$$

with each mode having its own unique exit impedance for no reflection.

In the numerical treatment, the boundary condition used at the duct exit $x = L$ was

$$\zeta_e = 2\pi\eta \frac{p}{u_x} = 1 \tag{E8}$$

where the numerical value of 1 indicates the condition for the case in which a plane one-dimensional pressure wave would not be reflected at the tube exit.

In comparing the exact analytical exit impedance conditions required for no reflection, equation (E6), to the numerical exit impedance condition, equation (E8), we are led to the conclusion that reflections are occurring at the duct exit in the numerical calculations. Choosing ζ_e equal to 1 in the numerical calculation cannot satisfy all the distinct

impedance values for each mode as given in equation (E6). Clearly, the analytical and numerical solutions for the attenuation in a duct of a given length will not be identical.

If we overlook roundoff and truncation errors in the numerical calculations, the attenuation calculated by the numerical technique will be greater than that calculated by the exact analytical technique because of reflections which occur at the exit; that is,

$$\Delta dB\Big)_{\substack{\text{numerical} \\ 0 \le x \le L}} \geq \Delta dB\Big)_{\substack{\text{analytical} \\ 0 \le x \le L}} \tag{E9}$$

The reflected energy appears to have been absorbed by the soft wall in the numerical calculation.

Fortunately, in many practical problems, most of the higher order modes decay out and only the lowest order mode appears at the exit. A comparison to the analytical results indicates that in general the exit impedance associated with the lowest order mode is close to ρc. Nevertheless, it is important to establish a general numerical procedure which will converge to the correct answer.

Consider the case where an additional length of absorbing liner ΔL is added to the original liner, so that the liner now has a length $L + \Delta L$. If ΔL is chosen sufficiently long, the reflected energy at the duct exit, $x = L + \Delta L$, will be absorbed before this energy can reach the previous exit position at $x = L$. Therefore, for soft-wall ducts

$$\lim_{\Delta L \to \infty} \Delta dB\Big)_{\substack{\text{numerical} \\ 0 \le x \le L}} = \Delta dB\Big)_{\substack{\text{analytical} \\ 0 \le x \le L}} \tag{E10}$$

Practically, the liner length need only be increased by some minimum length ΔL until the attenuation for the liner length between $x = 0$ and $x = L$ remains constant to a given percentage.

REFERENCES

1. Morse, Philip M.: The Transmission of Sound Inside Pipes. J. Acoust. Soc. Am., vol. 11, no. 2, Oct. 1939, pp. 205-210.

2. Cremer, Lothar: Theorie der Luftschall-Dämpfung in Rechteckkanal mit Schluckender Wand und das sich dabei Ergebende höchste Dämpfungsmass. Acustica, vol. 3, no. 2, 1953, pp. 249-263.

3. Rice, Edward J.: Attenuation of Sound in Softwalled Circular Ducts. Presented at the AFOSR-UTIAS Symposium on Aerodynamic Noise, Toronto, May 20-21, 1968.

4. Rice, Edward J.: Propagation of Waves in an Acoustically Lined Duct with a Mean Flow. Basic Aerodynamic Noise Research. NASA SP-207, 1969, pp. 345-355.

5. Eversman, Walter: The Effect of Mach Number on the Tuning of an Acoustic Lining in a Flow Duct. J. Acoust. Soc. Am., vol. 48, no. 2, pt. 1, 1970, pp. 425-428.

6. Tack, D. H.; and Lambert, R. F.: Influence of Shear Flow on Sound Attenuation in a Lined Duct. J. Acoust. Soc. Am., vol. 38, no. 4, Oct. 1965, pp. 655-666.

7. Pridmore-Brown, D. C.: Sound Propagation in a Fluid Flowing Through an Attenuation Duct. J. Fluid Mech., vol. 4, pt. 4, Aug. 1958, pp. 393-406.

8. Mungur, P.; and Gladwell, G. M. L.: Acoustic Wave Propagation in a Sheared Fluid Contained in a Duct. J. Sound Vib., vol. 9, no. 1, Jan. 1969, pp. 28-48.

9. Mungur, P.; and Plumblee, H. E.: Propagation and Attenuation of Sound in a Soft-Walled Annular Duct Containing a Shear Flow. Basic Aerodynamic Noise Research. NASA SP-207, 1969, pp. 305-327.

10. Hersh, A. S.; and Catton, I.: Effect of Shear Flow on Sound Propagation in Rectangular Ducts. J. Acoust. Soc. Am., vol. 50, no. 3, pt. 2, 1971, pp. 992-1003.

11. Eversman, Walter: Effect of Boundary Layer on the Transmission and Attenuation of Sound in an Acoustically Treated Circular Duct. J. Acoust. Soc. Am., vol. 49, no. 5, pt. 1, 1971, pp. 1372-1380.

12. Mariano, S.: Effect of Wall Shear Layers on the Sound Attenuation in Acoustically Lined Rectangular Ducts. J. Sound Vib., vol. 19, no. 3, Dec. 8, 1971, pp. 261-275.

13. Savkar, S. D.: Propagation of Sound in Ducts with Shear Flow. J. Sound Vib., vol. 19, no. 3, Dec. 8, 1971, pp. 355-372.

14. Shankar, P. M.: On Acoustic Refraction by Duct Shear Layers. J. Fluid Mech., vol. 47, pt. 1, May 14, 1971, pp. 81-91.

15. Ko, S.-H.: Sound Attenuation in Acoustically Lined Circular Ducts in the Presence of Uniform Flow and Shear Flow. J. Sound Vib., vol. 22, no. 2, May 22, 1972, pp. 193-210.

16. Shankar, P. N.: Sound Propagation in Duct Shear Layers. J. Sound Vib., vol. 22, no. 2, May 22, 1972, pp. 221-232.

17. Shankar, P. N.: Acoustic Refraction and Attenuation in Cylindrical and Annular Ducts. J. Sound Vib., vol. 22, no. 2, May 22, 1972, pp. 233-246.

18. Varga, Richard S.: Matrix Iterative Analysis. Prentice-Hall, Inc., 1962.

19. Moon, Parry; and Spencer, Domina E.: Field Theory for Engineers. D. Van Nostrand Co., Inc., 1961.

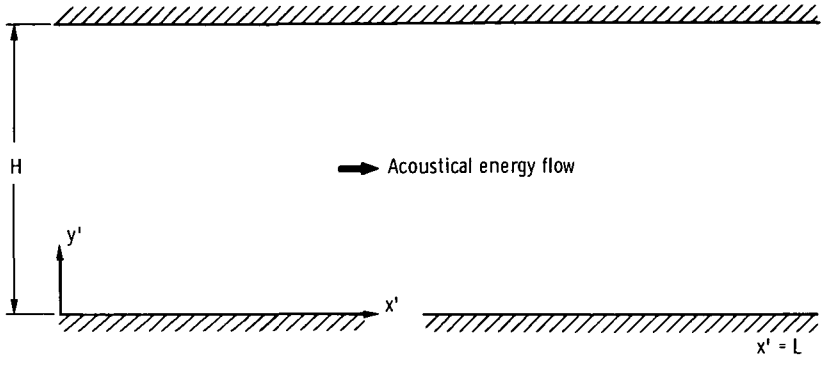

Figure 1. - Coordinate system for two-dimensional duct.

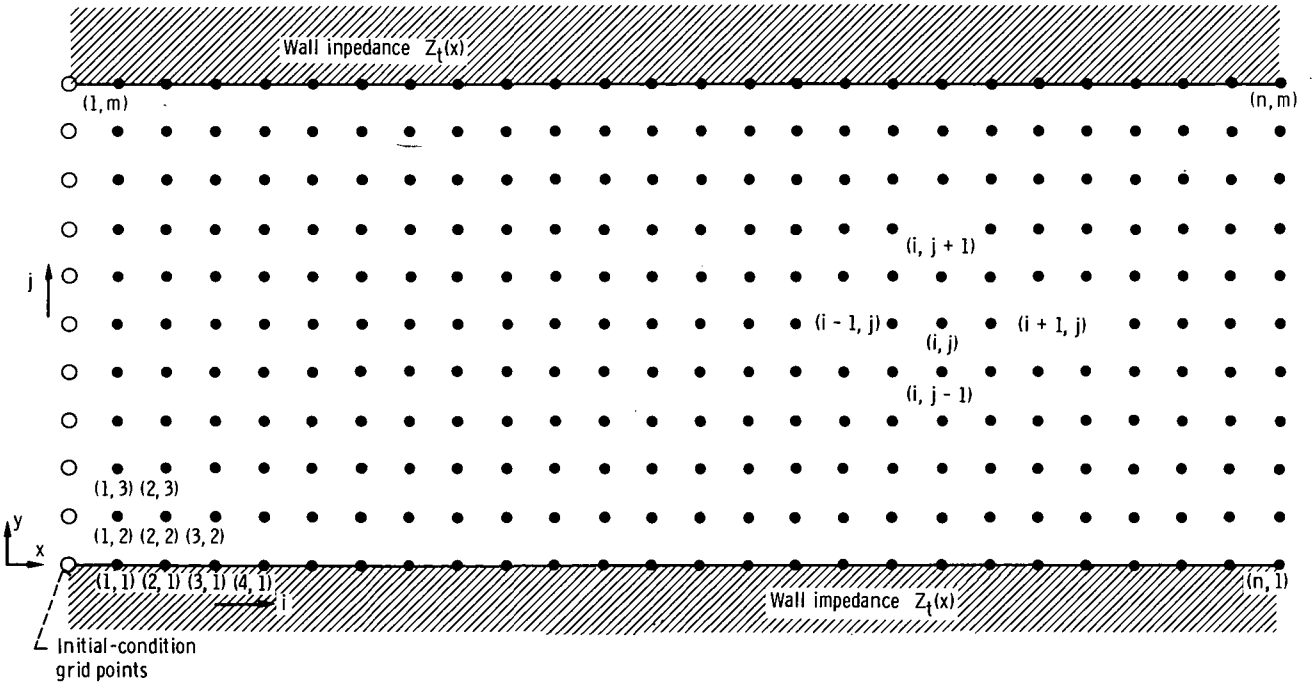

Figure 2. - Grid-point representation of two-dimensional flow duct.

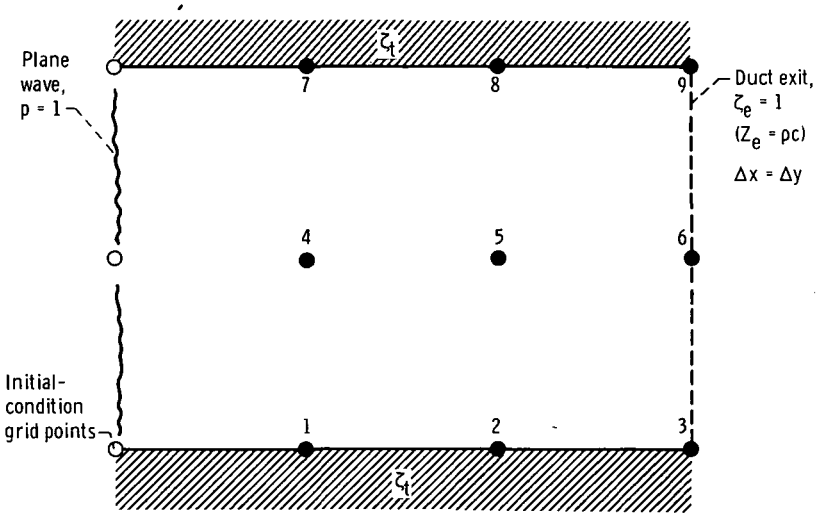

Figure 3. - Illustrative example of soft-wall duct with total number of grid rows m of 3 and total number of grid columns n of 3.

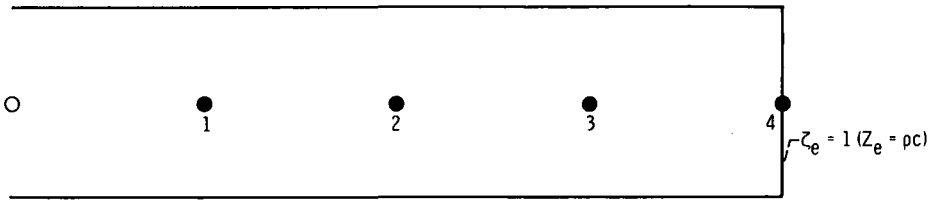

Figure 4. - One-dimensional sound propagation with no reflections.

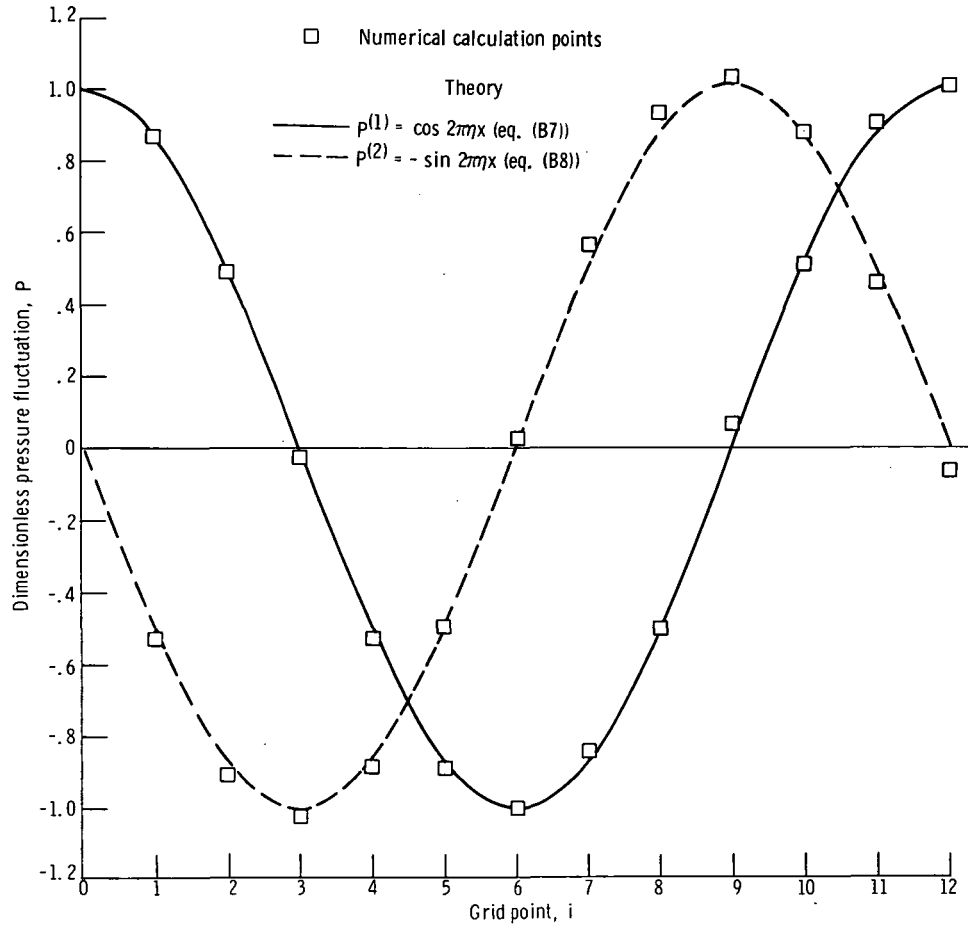

Figure 5. - Pressure profiles for one-dimensional sound propagation without reflections for dimensionless frequency η of 1 and number of grid columns n of 12.

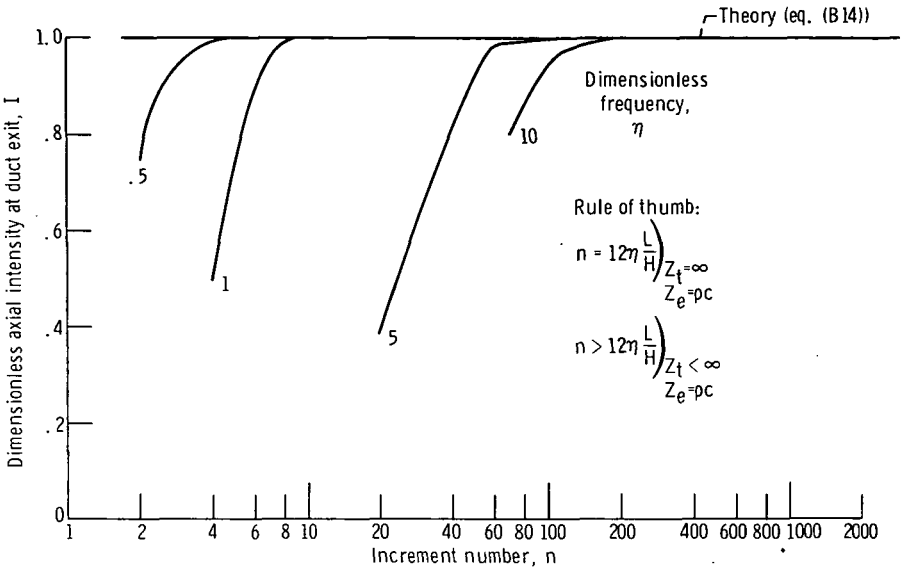

Figure 6. - Effect of increment number on calculated intensity of one-dimensional sound wave propagation without reflections.

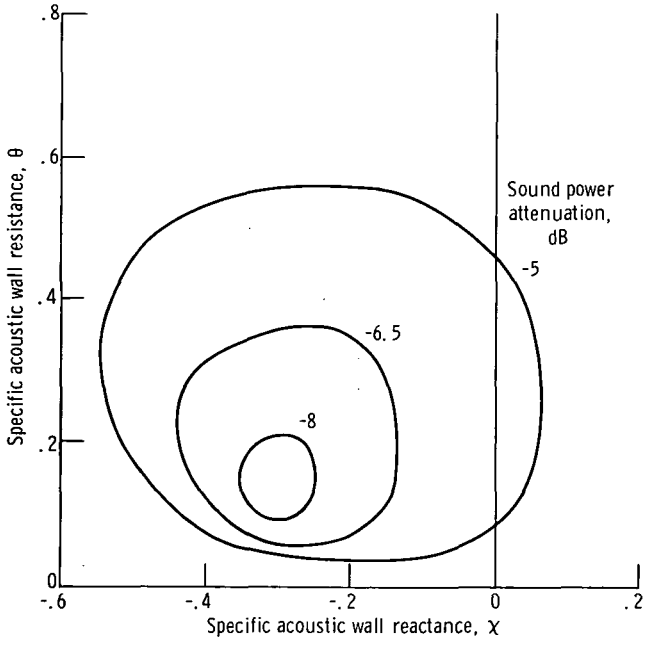

Figure 7. - Sound power attenuation contours for dimensionless frequency η of 0.6, length-height ratio L/H of 0.5, total number of grid rows m of 20 and total number of grid columns n of 5.

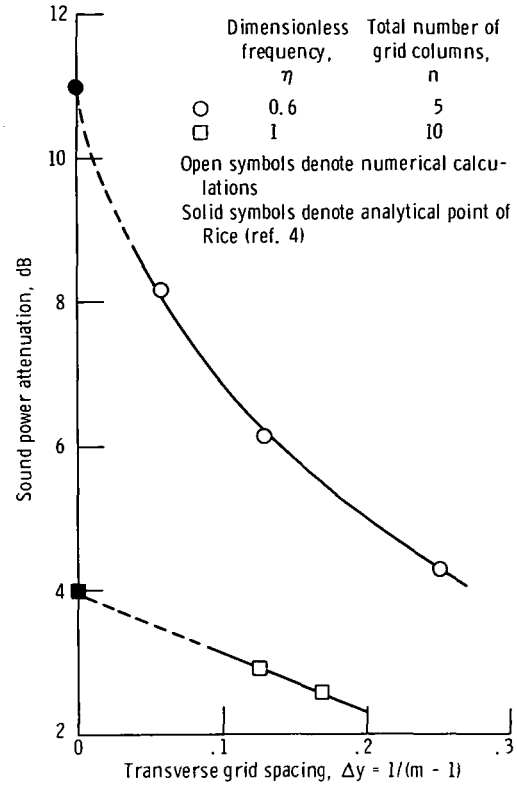

Figure 8. - Effect of spacing on attenuation at optimum impedance.

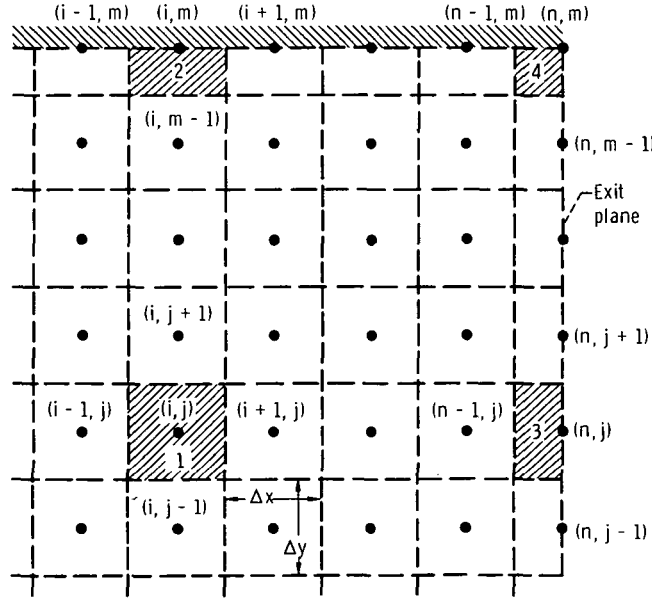

Figure 9. - Integration cells for establishing difference equations.

NASA-Langley, 1973 —— 28 E-7217

NATIONAL AERONAUTICS AND SPACE ADMINISTRATION
WASHINGTON, D.C. 20546

OFFICIAL BUSINESS
PENALTY FOR PRIVATE USE $300

SPECIAL FOURTH-CLASS RATE BOOK

POSTAGE AND FEES PAID
NATIONAL AERONAUTICS AND SPACE ADMINISTRATION
451

U.S.MAIL

POSTMASTER: If Undeliverable (Section 158 Postal Manual) Do Not Return

"The aeronautical and space activities of the United States shall be conducted so as to contribute . . . to the expansion of human knowledge of phenomena in the atmosphere and space. The Administration shall provide for the widest practicable and appropriate dissemination of information concerning its activities and the results thereof."

—NATIONAL AERONAUTICS AND SPACE ACT OF 1958

NASA SCIENTIFIC AND TECHNICAL PUBLICATIONS

TECHNICAL REPORTS: Scientific and technical information considered important, complete, and a lasting contribution to existing knowledge.

TECHNICAL NOTES: Information less broad in scope but nevertheless of importance as a contribution to existing knowledge.

TECHNICAL MEMORANDUMS: Information receiving limited distribution because of preliminary data, security classification, or other reasons. Also includes conference proceedings with either limited or unlimited distribution.

CONTRACTOR REPORTS: Scientific and technical information generated under a NASA contract or grant and considered an important contribution to existing knowledge.

TECHNICAL TRANSLATIONS: Information published in a foreign language considered to merit NASA distribution in English.

SPECIAL PUBLICATIONS: Information derived from or of value to NASA activities. Publications include final reports of major projects, monographs, data compilations, handbooks, sourcebooks, and special bibliographies.

TECHNOLOGY UTILIZATION PUBLICATIONS: Information on technology used by NASA that may be of particular interest in commercial and other non-aerospace applications. Publications include Tech Briefs, Technology Utilization Reports and Technology Surveys.

Details on the availability of these publications may be obtained from:

SCIENTIFIC AND TECHNICAL INFORMATION OFFICE

NATIONAL AERONAUTICS AND SPACE ADMINISTRATION

Washington, D.C. 20546